Available online at www.sciencedirect.com
SCIENCE DIRECT®
Journal of Nuclear Materials 321 (2003) 110–114
journal of nuclear materials
www.elsevier.com/locate/jnucmat

Letter to the Editors

Light emission from carbon-based materials under ITER relevant thermal shock loads

T. Hirai [a,*], J. Linke [a], W. Kühnlein [b], G. Sergienko [c], S. Brezinsek [c]

[a] *IWV 2, Forschungszentrum Jülich GmbH, EURATOM-Association, 52425 Jülich, Germany*
[b] *BZ Forschungszentrum Jülich GmbH, EURATOM-Association, 52425 Jülich, Germany*
[c] *IPP Forschungszentrum Jülich GmbH, EURATOM-Association, Trilateral Euregio Cluster, 52425 Jülich, Germany*

Received 28 January 2003; accepted 21 March 2003

Abstract

Light emission from carbon-based materials (fine grain graphite, CFC and silicon doped CFC) was observed during ITER relevant thermal shock loads by means of in situ optical diagnostics. The light emission which corresponds to particle release clearly indicated different particle release processes in the three materials. The differences were also found in the initiation temperatures of particle release and the surface morphology of the loaded areas. These results are related to the thermal stress in bulk materials. In addition to particle release, vapor cloud formation caused by thermal shock loads were observed as CII lines and lines from the C_2 Swan system. No Si lines but lines from SiC_2 molecules (Merrill–Sanford bands) were observed in Si doped CFC. This indicates that atomic silicon is not released under ITER relevant thermal shock loads.

1. Introduction

Thermal shock loads of the order of a few 10 MJ/m^2 in several ms (disruptions) and about 60 MJ/m^2 in several hundred ms (vertical displacement events (VDEs)) are expected in the International Thermonuclear Experimental Reactor (ITER) [1]. Armor materials will be strongly eroded under these conditions, therefore, the materials' R&D under these transient power loads still remains as one of the most challenging issues associating with the lifetime of the armor materials.

Since carbon-based materials have a high thermal shock resistance and, additionally, carbon fiber composites (CFCs) show high thermal conductivity (up to 350 W/m K), they were selected as candidate plasma facing armor materials in ITER [2]. However, recent studies show a strong erosion of carbon-based materials due to particle release (Fig. 1) caused by brittle destruction during thermal shock loads [3–7]. Therefore, it is important to study the material behavior under intense thermal loads.

In the present work, the light emission from carbon-based materials was studied by optical diagnostics under ITER relevant disruption conditions.

2. Experimental

ITER relevant thermal shock loads were applied with an energetic electron beam in the electron beam facility, JUDITH. The details of the facility are described elsewhere [8]. Three carbon-based materials: fine grain graphite (R6650, SGL Carbon-Ringsdorff), CFC (NB31, SNECMA Motors) and silicon doped CFC (NS31, SNECMA Motors) with dimensions of $25 \times 25 \times 10$ mm^3, were loaded by electron beam (120 keV, $\Phi \approx 1$ mm) at room temperature in vacuum ($<10^{-4}$ Pa).

* Corresponding author. Tel.: +49-2461 615843; fax: +49-2461 613699.
E-mail address: t.hirai@fz-juelich.de (T. Hirai).

0022-3115/$ - see front matter © 2003 Elsevier B.V. All rights reserved.
doi:10.1016/S0022-3115(03)00198-3

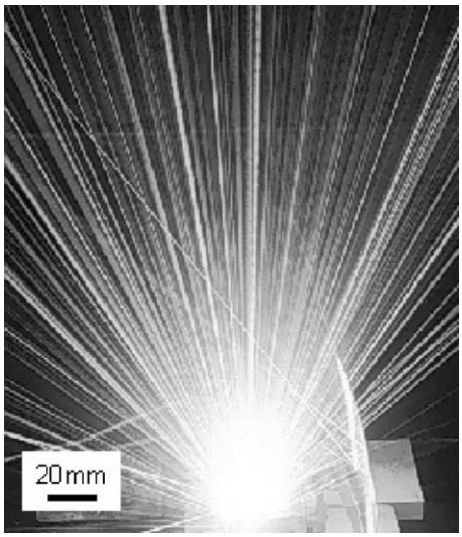

Fig. 1. Particle release from fine grain graphite during a thermal shock load (4.8 GW/m^2, 5 ms, RT) [4].

The silicon doped CFC contains 8–10% silicon in the bulk material [2]. The loaded power density, the duration and the loaded area were 2.2 GW/m^2, 4.6 ms and 4×4 mm^2, respectively.

During power loading, the light emission was observed by a spectrometer in the visible range (HS2000, Avantes), a photodiode (HFD-1100, Laser Components) and a pyrometer (Kleiber 273, Kleiber) (Fig. 2). Using the spectrometer, light emission in the wavelength range between 350 and 800 nm was observed within a line integral observation volume, 3 mm from the surface ($\Phi \approx 10$ mm). The photodiode (silicon photodiode: the maximum sensitivity around 900 nm) which was used to measure visible and infrared light, had a line integral observation volume at 10 mm above the surface with viewing angle of 30° ($\Phi \approx 3$ mm). The pyrometer was pointing at the loaded hot surface with an observation area of $\Phi \approx 4$ mm. The spectrometer had a time resolution of 100 ms, which allowed the observation of time-integrated spectra during the power loads (4.6 ms), whereas the other diagnostics with a time resolution of 1 μs allowed monitoring the time evolution of light emission and surface temperature. In addition to the optical measurements, the absorbed current (electric current through the samples) was monitored by measuring the electric potential of a grounded resistor (100 Ω) with a time resolution of 1 μs (Fig. 2).

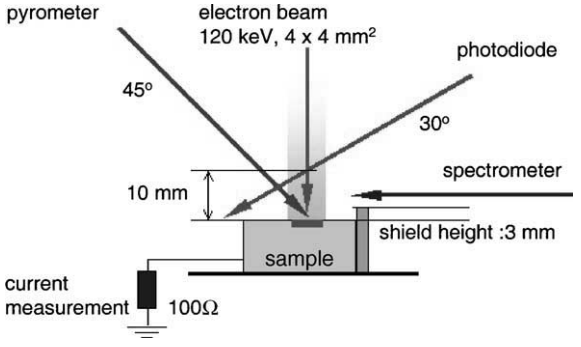

Fig. 2. Schematic view of the experimental setup.

3. Results and discussion

The light emission detected by the photodiode, surface temperature measured by the pyrometer (emissivity: 0.9) and absorbed current are shown in Fig. 3. Spikes as marked in Fig. 3(a) as 'A' were observed in the photodiode signal. The spike indicates that a bright light source, i.e. a hot particle, passed through the observation volume. In the experiments, the hot particles are the

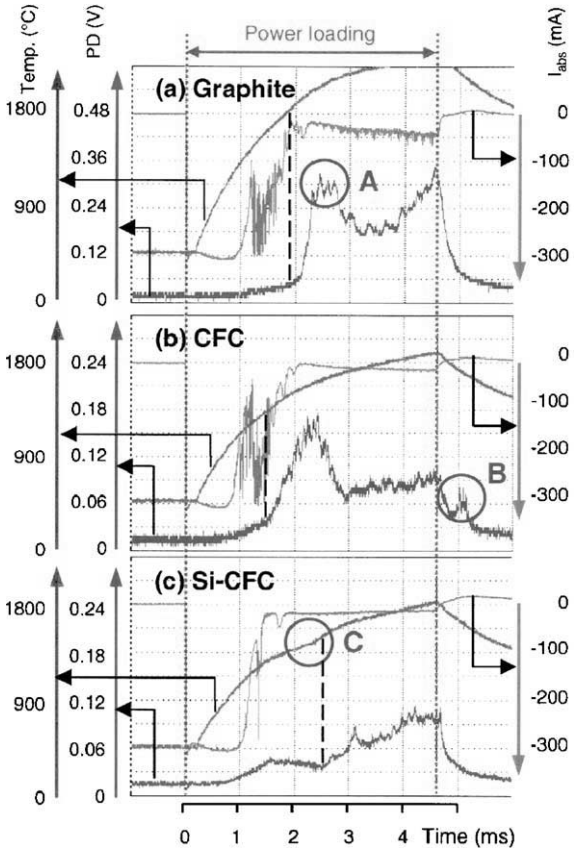

Fig. 3. Surface temperature, light emission detected by photodiode and absorbed current during thermal shock loads (2.2 GW/m^2, 4.6 ms, RT): (a) fine gain graphite, (b) CFC and (c) Si doped CFC. A: Spikes in the photodiode signal in graphite. B: Particle release (light emission) in the cooling phase in CFC. C: Stagnation point of the surface temperature in Si doped CFC.

particles released due to brittle destruction [3–6]. It should be noted that the intensity of the detected light depends on the temperature, the size and the number of particles, therefore, it is not straightforward to quantify the signals. However, the signal defines the initiation of the particle release. The particle release from graphite is correlated with the absorbed current signal and occurs always in the last plateau regime of the absorbed current (after 2.2 ms in this particular case). The particle release starts at 1800 °C (shown as a dashed line in Fig. 3(a)). This temperature was independent of the heating rate (i.e. incident power density). Accordingly, it is concluded that particle release originates from the thermal stress during thermal shock loads.

In case of CFC and Si doped CFC, the initiation temperatures were obviously different, at 1300 °C for CFC and 1500 °C for Si doped CFC (shown as dashed lines in Fig. 3(b) and (c)), respectively. These results show that the particle release processes were different among the three materials. In fact, the surface morphology of the loaded samples indicates different erosion mechanisms (shown in Fig. 4). Rather homogeneous erosion with no clear crater formation was observed in graphite (Fig. 4(a)), whereas strong erosion along horizontally arranged fibers (PAN fibers) was observed in CFC and Si doped CFC (indicated in Fig. 4(b) and (c) as 'A'). Accordingly, particle release was initiated at horizontally arranged fibers in cases of CFC and Si doped CFC. The fibers were overheated under thermal shock loads because they have a low thermal conductivity in the perpendicular direction to the surface. The lower initiation temperature of particle release originated from the heterogeneous microstructure of the CFCs. The area observed by the pyrometer was in the area of $\Phi \approx 4$ mm, which contained horizontally arranged fibers with a low heat removal potential and vertically arranged fibers (pitch fibers) with a high heat removal potential. Consequently, the average surface temperature has been measured. The particle release started at locally overheated fibers, i.e. the horizontally arranged fibers.

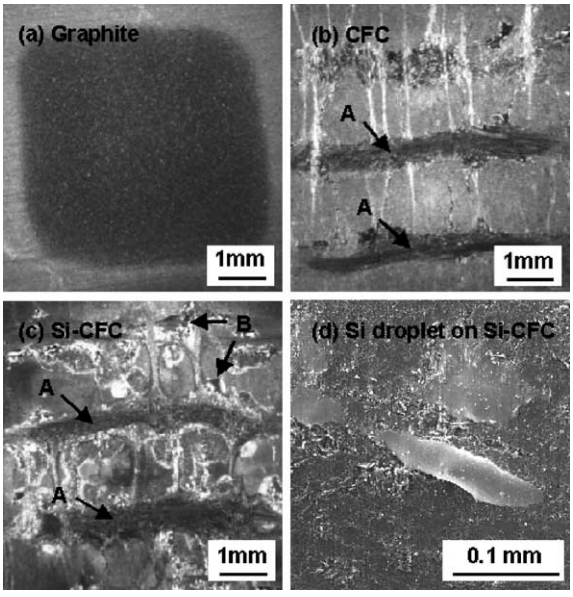

Fig. 4. Surface morphology of loaded samples (2.2 GW/m^2, 4.6 ms, RT): (a) fine grain graphite, (b) CFC, (c) Si doped CFC and (d) Si droplet on the surface of Si doped CFC. A: Strong erosion along horizontally arranged fiber in CFC and Si doped CFC. B: Silicon segregations at the top surface of the Si doped CFC.

The photodiode signals show a different behavior: a fairly flat profile in graphite, a plateau after a large peak in CFC and small spikes and a peak after a plateau in Si doped CFC. The time evolutions also show the different particle release processes. The details of the individual particle release processes are still under discussion. The particle release after the power loading, i.e. in the cooling phase was observed in CFC (marked in Fig. 3(b) as 'B'). The surface temperature started to decrease and the surface stress originated from temperature gradient began to change compressive stress into tensile stress. During this process, the surface temperature was still high enough to release hot particles. This result is consistent with the interpretation mentioned above: the contribution of thermal stress on brittle destruction. Another interesting result is the presence of a stagnation point of the surface temperature in Si doped CFC (marked in Fig. 3(c) as 'C'). This temperature was around 1450 °C which corresponds to the melting point of silicon (1414 °C). In fact, molten silicon was clearly observed as silicon segregation on the top surface (indicated as 'B' in Fig. 4(c)) and silicon droplets observed in the surrounding area (Fig. 4(d)).

The thermal shock loading experiments were performed at room temperature so far. At elevated temperature, the surface temperature will reach the initiation temperature in a shorter time and the particle release will start earlier. However, from the other point of view, the particle release can be moderated by the reduction of the thermal stress due to the less thermal gradient in pre-heated samples. Studies of brittle destruction at elevated temperatures are also important and interesting topics. Thermal shock loads on pre-heated samples are planned in the next campaign.

Emission spectra from the three materials during thermal shock loads are depicted in Fig. 5. The spectra were shown after background subtraction of thermal radiation caused by light reflection from the hot surface and hot particles passing through the observation volume. CII lines (426 and 589 nm) and the C_2 Swan system ($\Delta v = -2, -1, 0, 1, 2$) [9–11] were observed ($\Delta v = 2$ was clear only in the graphite sample). This is a clear

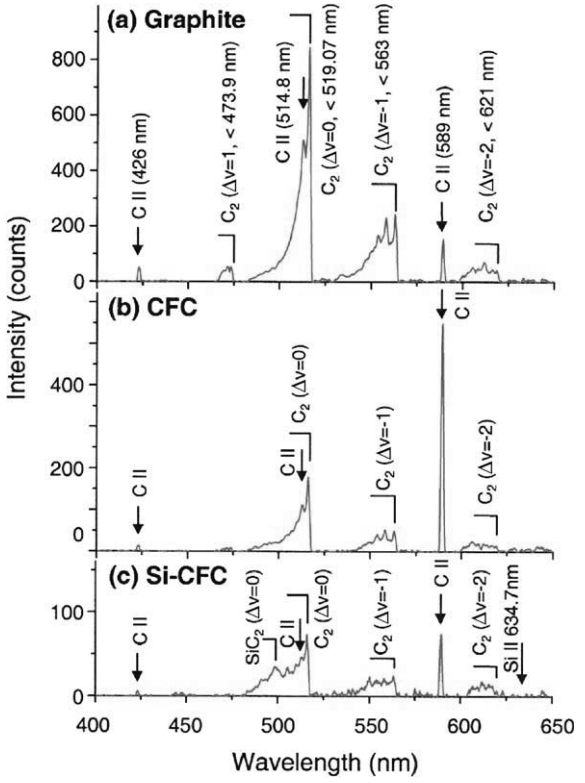

Fig. 5. Emission spectra from carbon-based materials during thermal shock loads (2.2 GW/m^2, 4.6 ms, RT): (a) fine grain graphite, (b) CFC and (c) Si doped CFC.

indication for the formation of ionized vapor clouds in front of the surfaces. It should be noted that the intensity and the intensity ratio were strongly dependent on the materials. The C_2 Swan system was dominant in graphite, whereas lines from carbon ions were dominant in CFC and Si doped CFC. The line intensity ratio, e.g. [CII (426 nm)] vs. [CII (589 nm)], was estimated to be 0.37 in graphite, whereas 0.03 in CFC and 0.07 in Si doped CFC. These results imply that the plasma parameters of the ionized vapor clouds in front of graphite were completely different from those detected in CFC and Si doped CFC [12].

Silicon lines were not observed in Si doped CFC (a representative Si II line in the visible range (635 nm) [13] is marked in Fig. 5(c)), even though silicon was segregated at the top surface and silicon droplets were observed on the top surface (Fig. 4(c) and (d)). The only silicon related lines which have been observed, were lines from SiC_2 molecules (Merrill–Sanford bands) around 497.7 nm [9,14]. There might be line emission from Si_2 molecules, however, bright lines from the molecules exist in the ultraviolet (UV) region that is outside of the observation wavelength range. Observation of the wider wavelength range from UV to infrared (IR) is planed in the next campaign. It is not clear why no Si II lines but lines from SiC_2 molecules were observed in these particular thermal shock loads. Nevertheless, it can be concluded that atomic silicon is not released into the ionized vapor cloud under ITER relevant thermal shock loads, even though silicon droplets will be ejected into the surroundings.

4. Summary

Optical diagnostics during thermal shock events were successfully installed in the electron beam facility JUDITH. Particle release was detected by means of a photodiode and a vapor cloud was observed by means of an emission spectrometer.

The initiation temperature of particle release depends on the surface temperature but not the heating rate (incident power density). In addition, particle release in the cooling phase was observed in CFC. The particle release due to brittle destruction is related to the thermal stress in the materials. Initiation temperatures of particle release were dependent on the materials, 1800 °C for graphite, 1300 °C for CFC and 1500 °C for Si doped CFC. The time evolutions of light emission showed that the particle release processes were different in the three materials.

Vapor clouds were observed by means of the detection of CII lines and lines from the C_2 Swan system. The intensity ratio of lines indicated that the plasma parameters of the ionized vapor clouds were dependent on the materials. No silicon lines but lines from SiC_2 molecules (Merrill–Sanford bands) were observed. This indicates that atomic silicon is not released under ITER relevant thermal shock loads.

References

[1] G. Federici, C.H. Skinner, J.N. Brooks, J.P. Coad, C. Grisolia, A.A. Haasz, A. Hassanein, V. Philipps, C.S. Pitcher, J. Roth, W.R. Wampler, D.G. Whyte, Nucl. Fus. 41 (2001) 1967.

[2] V. Barabash, M. Akiba, J.P. Bonal, G. Federici, R. Matera, K. Nakamura, H.D. Pacher, M. Rödig, G. Vieider, C.H. Wu, J. Nucl. Mater. 258–263 (1998) 149.

[3] J. Linke, E. Berthe, S. Amouroux, Y. Koza, W. Kühnlein, M. Rödig, in: 22th SOFT, 2002, Helsinki, Finland, to be published.

[4] J. Linke, M. Akiba, R. Duwe, A. Lodato, H.-J. Penkalla, M. Rödig, K. Schöpflin, J. Nucl. Mater. 290–293 (2001) 1102.

[5] J. Linke, H. Bolt, R. Duwe, W. Kühnlein, A. Lodato, M. Rödig, K. Schöpflin, B. Wiechers, J. Nucl. Mater. 283–287 (2000) 1152.

[6] J. Linke, R. Duwe, A. Gervash, R.H. Qian, M. Rödig, A. Schuster, J. Nucl. Mater. 258–263 (1998) 634.

[7] S. Pestchanyi, H. Würz, Phys. Scripta T 91 (2001) 84.
[8] R. Duwe, W. Kühnlein, H. Münstermann, in: 18th SOFT, 1994, p. 355.
[9] R.W.B. Pearse, A.G. Gaydon, The Identification of Molecular Spectra, Wiley, New York, 1976.
[10] T. Shinozaki, T. Ooie, T. Yano, J.P. Zhao, Z.Y. Chen, M. Yoneda, Appl. Surf. Sci. 197&198 (2002) 263.
[11] S. Arepalli, C.D. Scott, Chem. Phys. Lett. 302 (1999) 139.
[12] R.K. Janev, H.W. Drawin, Atomic and Plasma–Material Interaction Process in Controlled Thermonuclear Fusion, Elsevier, Amsterdam, 1993, p. 213.
[13] A. Huber, I. Beigman, D. Borodin, Ph. Mertens, V. Philipps, A. Pospieszczyk, U. Samm, B. Schweer, G. Sergienko, L. Vainshtein, Plasma Phys. Control. Fus. 45 (2003) 89.
[14] P.J. Sarre, M.E. Hurst, T. Lloyd Evans, The Astrophys. J. 471 (1996) L107.